Utrecht University Repository

Title	Thermal alteration of the aliphatic biopolymer cutan: implications for composition and degradation
Authors	Nierop, Klaas G.J.; Kaal, Joeri
Published in	Organic Geochemistry
Publication Date	2026-04
Link	https://dspace.library.uu.nl/handle/1874/480690
Citation	Nierop, K G J & Kaal, J 2026, 'Thermal alteration of the aliphatic biopolymer cutan : implications for composition and degradation', Organic Geochemistry, vol. 214, 105149. https://doi.org/10.1016/j.orggeochem.2026.105149
Versions / License	Publisher version
Rights	https://www.uu.nl/en/university-library/license-and-reuse-conditions

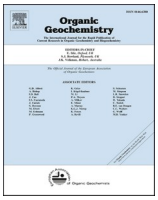
Organic Geochemistry 214 (2026) 105149



Contents lists available at ScienceDirect

Organic Geochemistry

journal homepage: www.elsevier.com/locate/orggeochem



Thermal alteration of the aliphatic biopolymer cutan: implications for composition and degradation

Klaas G.J. Nierop [a,*], Joeri Kaal [b]

[a] Geolab, Faculty of Geosciences, Utrecht University, Princetonlaan 8, 3584 CB Utrecht, the Netherlands
[b] Pyrolyscience, 15707 Santiago de Compostela, Spain

ARTICLE INFO

Associated editor: Mark Fitzsimons

Keywords:
Cutan
Charring
Extraction
Curie point pyrolysis
Thermally assisted hydrolysis and methylation

ABSTRACT

Cutan is the operationally defined residual fraction of cuticles after solvent extraction and hydrolysis. We investigated the thermal behaviour as a consequence of charring experiments of cutan isolated from *Agave americana* and *Clivia miniata*. While both cutan fractions exhibited almost identical weight loss patterns as a function of charring temperature, the molecular degradation and transformations differed, mainly reflected by higher carboxylic acid contents released and retained in the cutan residues of *C. miniata*, whereas cutan of *A. americana* comprised and released more hydroxy-containing moieties. The extractable fractions after charring yielded initially the building blocks of cutan, but with progressive heating defunctionalisation (removal of hydroxy and carboxylic acid groups) mainly *n*-1-alkenes and *n*-alkanes were produced. The lack of polyaromatic condensation products upon charring indicates the highly saturated character of cutan under severe conditions.

1. Introduction

Cuticles comprise the protective layer of higher plants. They minimize water loss and mechanical damage, and have several other functions (Leide et al., 2020). From a chemical point of view, they are composed of extractable cuticular waxes and a polymeric matrix known as cutin. The wax layer may consist of a larger variety of components: *n*-alkanes, primary and secondary alkanols, fatty acids, aldehydes, wax esters in the form of a combination of an alkanol and a fatty acid moiety, and terpenoids including sterols (Walton, 1990). Cutin is a biopolyester primarily build from C_{16} and C_{18} ω-hydroxy fatty acids with and without mid-chain functionalities such as hydroxy and epoxy groups enabling the formation of a crosslinked network (Kolattukudy, 2001).

Sometimes a residue remains after extraction of cuticles to isolate the waxes and the removal of cutin through hydrolysis. This operationally defined non-extractable, non-hydrolysable fraction has been termed non-ester cutin for *Clivia miniata* Reg. (Schmidt and Schönherr, 1982), and cutan in case of *Agave americana* L. (Nip et al., 1986a; 1986b). Although the chemical isolation approach between the aforementioned two works differed, Leide et al. (2020) showed that both plants contain such a non-hydrolysable, aliphatic biopolymer resisting exhaustive extraction and hydrolysis, whereas cuticles of *Ficus elastica* and *Prunus laurocerasus* were devoid of a cutan fraction, despite of earlier results using milder isolation approaches (Gouret et al., 1993; Guzmán-Delgado et al., 2016). It has been proposed that drought adapted plants with succulent leaves containing thick cuticles such as certain CAM plants contain cutan to help minimizing water loss via evaporation (Boom et al., 2005).

Due to its chemical resistance, a high preservation potential of cutan in the fossil record has been proposed (Tegelaar et al., 1989a; Boom et al., 2005). In addition, artificial maturation of isolated *A. americana* cutan generated a high-wax crude oil (Tegelaar et al., 1989b). Cutan is also found to be a very effective sorbent of organic components in soil (Shechter et al., 2010). Together this implies that the thermal behaviour of cutan is relevant to understand its fate as a potential long-term carbon source as well as during its management to form a stable plant residue (biochar, compost). While the chemical structure of cutan is highly enigmatic and supposed to comprise of long aliphatic chains with minor amounts of aromatic moieties bound via non-hydrolysable ester and/or ether bonds (Schouten et al., 1998; Deshmukh et al., 2005), a close relationship between the cuticular wax compounds and cutan monomers (*n*-alkanols, α,ω-alkanediols, fatty acids, ω-hydroxy fatty acids) in the C_{28}-C_{34} range was observed by Leide et al. (2020). This observation was based on thermally assisted hydrolysis and methylation (THM) of cutan obtained from *A. americana* only as its building blocks were relatively efficiently released. By contrast, this was possible to a limited extent

* Corresponding author.
E-mail address: k.g.j.nierop@uu.nl (K.G.J. Nierop).

https://doi.org/10.1016/j.orggeochem.2026.105149
Received 20 October 2025; Received in revised form 14 January 2026; Accepted 29 January 2026
Available online 31 January 2026
0146-6380/© 2026 The Author(s). Published by Elsevier Ltd. This is an open access article under the CC BY license (http://creativecommons.org/licenses/by/4.0/).

only for cutan of *C. miniata* due to competing flash pyrolysis mechanisms, likely due to the poor interaction between tetramethylammonium hydroxide and the hydrolysable bonds (Leide et al., 2020). As a consequence, the composition of cutan of *C. miniata* remains, yet, unresolved.

As a follow-up of the study by Leide et al. (2020), in the present study an artificial heating procedure, sometimes referred to as 'charring', is applied to cutan obtained from both *A. americana* and *C. miniata* to examine their thermal degradation patterns. This procedure comprises heating under low oxic conditions at temperatures ranging, in our study, between 200 and 600 °C (Hall et al., 2008; Kaal et al., 2012a). As a result, thermal barriers are lost at the lower temperatures (200–350 °C) releasing the more weaker bound building blocks from the polymeric matrix, while at temperatures of 400 °C and above charring reactions (loss of thermolabile functional groups and finally condensation into a polyaromatic network) are expected to dominate (Kaal and Calvelo-Pereira, 2016). The soluble compounds released after this heating were examined as well as their solid residues using flash pyrolysis and THM. As a result, this approach allows for a 'double shot' thermal degradation sequence to assess both the composition, in particular by the compounds released after the first shot, and thermal behaviour of cutan upon the second shot.

2. Materials and methods

2.1. Isolation of cutan

Agave americana and *Clivia miniata* plants were cultivated in a growth chamber with 75% relative humidity, a 14 h photoperiod at 450 μmol photons m^{-2} *s^{-1}, and a temperature regime of 22/18 °C (day/night) in the Botanic Garden of Wurzburg. Fully expanded leaves were investigated (Leide et al., 2020). Cuticles were provided by Jana Leide (University of Würzburg) and isolated from *A. americana* and *C. miniata* leaves according to the procedure described previously (Leide et al., 2020). Subsequently, cuticles were Soxhlet extracted by a mixture of dichloromethane-methanol (7.5:1, v/v) for 24 h. After air-drying, base hydrolysis, using 2 M KOH in 96% methanol at 70 °C for 4 h, was conducted on the residual cuticular material. Prior to acidification of the reaction mixture with 2 M HCl, it was allowed to cool down. Next, dichloromethane was added to remove any cutin monomer by liquid–liquid extraction. This process was repeated twice. The remaining solid residue was air-dried. To investigate possible involvement of methanol in the formation of thermal products, ethanol instead of methanol was used to prepare cutan from cuticles from both species as well.

2.2. Heating experiments

Between 5 and 44 mg of cutan aliquots were double-wrapped in aluminium foil to avoid air exposure and placed in a Lenton ECF muffle furnace for 30 min (Hall et al., 2008; Kaal et al., 2012a). The furnace was pre-heated at a temperature ranging between 200 °C and 500 °C, at 50 °C intervals, and 600 °C. No residue was obtained after charring at 500 °C, possibly because of occurrence of combustion conditions (cracked foil). Weight loss was determined gravimetrically. The cutan fraction obtained when using ethanol was charred only at 300 °C to test the involvement of methanol and ethanol respectively in the thermally formed products. Based on the results of methanol-based cutan we choose to use the heating at 300 °C as this is the lowest temperature at which the complete suite of products was formed.

2.3. Extraction and workup of lipids from heated cuticles

Heated cuticles were ultrasonically extracted using dichloromethane-methanol (9:1, v/v) for 15 min. The solvent mixture was removed from the solid material using a Pasteur pipette and allowed to pass a sodium sulfate column to remove solid particles and any trace of water. This procedure was repeated four times. The combined dichloromethane-methanol phases were dried under a gentle stream of nitrogen gas. The dried extracts were methylated using trimethylsilyldiazomethane. The methylated extracts were subsequently fractionated over an aluminium oxide column to obtain non-polar (i.e., hydrocarbons), neutral (i.e., ketones and methylated fatty acids) and polar (all hydroxy-containing hydrocarbons) fractions using hexane: dichloromethane (9:1, v/v), hexane:dichloromethane (1:1, v/v), and dichloromethane:methanol (1:1, v/v), respectively. Each fraction was dried under a gentle stream of nitrogen. Prior to analysis, polar fractions were derivatized using *bis*(trimethylsilyl)trifluoracetamide in pyridine at 60 °C for 20 min to convert hydroxy groups into the corresponding trimethylsilyl ethers. After cooling down, polar fractions were dried using a gentle stream of nitrogen.

Double bond positions in alkenes were determined by dissolving the non-polar fraction in 100 μL of hexane, after which 20 μL of a 60 mg mL^{-1} solution of iodine in diethyl ether and 100 μL of dimethyl disulfide were added. Samples were incubated in an oven at 40 °C and allowed to react overnight. After cooling down, the remaining iodine was removed using sodium thiosulfate in water. After removal of the organic layer, the aqueous phase was extracted two additional times with hexane. Subsequently, the combined *n*-hexane phase was passed over a small sodium sulfate column to remove any water. The resulting organic phase was dried under a gentle stream of nitrogen and subsequently redissolved in hexane prior to analysis.

2.4. Gas chromatography–flame ionization detector (GC–FID) and gas chromatography–mass spectrometry (GC–MS)

Non-polar fractions were re-dissolved in hexane, whereas both neutral and polar fractions were taken into ethyl acetate. Fractions were on-column injected on a Hewlett Packard 6890 Gas Chromatograph – Flame Ionization Detector (GC–FID) and a Agilent 7890B GC coupled to a 5977B MSD (Agilent Technologies) onto a CP-Sil 5CB fused silica column (30 m x 0.32 mm i.d., film thickness 0.10 μm). The GC–FID was operated at constant pressure of 100 kPa, whereas the GC–MS was operated at constant flow of 1.0 ml/min. Helium was used as carrier gas. The oven of both GC's was programmed starting at 70 °C to rise to 130 °C at a rate of 20 °C min^{-1}, and then to 320 °C at a rate of 4 °C min^{-1}, followed by an isothermal hold for 20 min. The GC–MS operated within a scanning range of *m/z* 50–800 (ionization energy 70 eV, cycle time 0.5 s). A known amount of squalane was used as a standard for quantification and was co-injected together with each fraction (1 μL of a ~2 μg $μL^{-1}$ solution).

2.5. Pyrolysis-gas chromatography-mass spectrometry (Py–GC–MS) and thermally assisted hydrolysis and methylation (THM) –GC–MS of residues after extraction

Flash pyrolysis was carried out on a Horizon Instruments Curie Point pyrolyser. Samples (approximately 0.5 mg) were pressed onto Ni/Fe Curie point wires and subsequently heated for 5 s at 600 °C. The pyrolysis unit was connected to a GC8060 Gas Chromatograph (Carlo Erba) and the products were separated by a fused silica column (J&W VF-1 ms, 25 m, 0.32 mm i.d.) coated with 100% dimethylpolysiloxane (film thickness 0.40 μm). Helium was used as carrier gas. The GC column was directly connected to the pyrolysis unit through a splitless injector set at 280 °C. The oven was initially kept at 40 °C for 1 min, next it was heated at a rate of 7 °C min^{-1} to 320 °C and maintained at that temperature for 15 min. The column was coupled to a MD800 mass spectrometer (Fisons; mass range *m/z* 45–650, ionization energy 70 eV, cycle time 0.7 s).

THM, i.e. rapid heating in the presence of tetramethylammonium hydroxide was employed to provide more insight in the presence of polar functional groups. With THM, hydrolysable ester bonds are cleaved and the resulting carboxylic acid and hydroxyl groups are transformed *in situ* to the corresponding methyl esters and methyl ethers,

respectively (Challinor, 2001). In addition, free carboxylic acid and hydroxyl groups will be methylated. Prior to THM, a droplet of a 25% solution of tetramethylammonium hydroxide in water was added to the samples pressed onto 350 °C Curie point wires, which were subsequently dried under a 100 W halogen lamp. Analysis of the THM products by way of GC–MS was performed similar to the conditions used for conventional pyrolysis. Identification of the compounds was carried out by their mass spectra using a NIST library or by interpretation of the spectra, by their retention times and/or by comparison with literature data.

2.6. Statistical analysis

The principal components analysis (PCA) function of the Tanagra open source software package (Rakotomalala, 2005) was performed for dimensionality reduction of the compounds identified in extracts, pyrolysates and THM products. We used relative proportions of individual compounds as input variables. No factor rotation was applied, and we focus on the first three component (PC1-PC3).

3. Results

3.1. Weight loss

Weight loss as a function of heating temperature ranged from 4.0% at 200 °C to 88–89% at 600 °C, independent of species (Fig. 1). Relatively large increments in weight loss were found between 400 °C and 450 °C, and between 450 °C and 600 °C. In addition to the solid residue that was used for analysis, a yellowish tar deposit was formed at 400 °C and higher, for both species. In fact, for the chars obtained at 450 °C the amount of tar was considerable and at 600 °C all residue consisted of tar (no solid residue available for analysis).

3.2. Thermally released extractable building blocks

Summed concentrations of all thermally treated and subsequently extractable lipids (*n*-alkanols, α,ω-alkanediols, fatty acids, α,ω-alkanedioic acids, ω-hydroxy fatty acids, 9,10,18-trihydroxy C_{18} fatty acid, 2-methylketones, *n*-alkenes and *n*-alkanes) showed a slight decrease from 200 °C to 250 °C for *C. miniata*, and a more distinct decline from 200 to 300 °C for *A. americana*, after which the yields increased to 450 °C (Fig. 2). For *A. americana* a second order polynomial regression curve with an $R^2 = 0.967$ described its lipid release as a function of charring. By contrast, an exponential increase with $R^2 = 0.93$

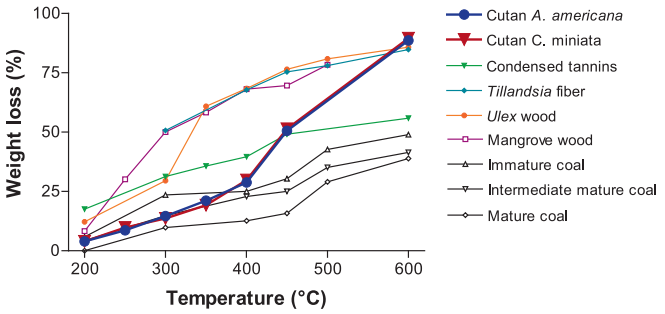


Fig. 1. Weight loss during experimental charring plotted against highest treatment temperature of cutan fractions of A. americana (●) and C. miniata (▼). For comparison, experimental chars of other materials produced under the same conditions are shown: condensed tannins from Pinus nigra needles (Kaal et al., 2012b), Tillandsia osneoides fibre (Kaal and Gilmore, 2018), wood from Ulex europaeus and mangrove (Kaal et al., 2012a), and a series of coal samples from Borneo, i.e., an immature coal from Balingian (%Ro ~ 0.31), a coalfield with intermediate maturity from Mukah (%Ro ~ 0.37) and mature coal from Pinangah (%Ro ~ 0.55; Kaal et al., 2017).

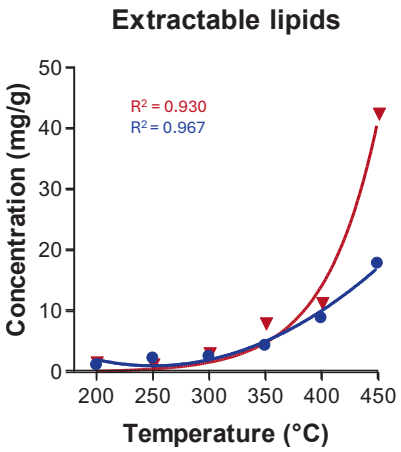


Fig. 2. Sum of all extractable components released from cutan *A. americana* (●) and *C. miniata* (▼) as a function of charring temperature.

reflects the lipids released for *C. miniata* best.

While *A. americana* was much richer in *n*-alkanols (C_{22}-C_{34}) than *C. miniata*, both species showed the same tendency with decreasing absolute and relative concentrations from 200 °C to 400 °C, whereas *n*-alkanols were absent at higher temperatures (Fig. 3, Table 1 for concentrations of each compound group, and Suppl. Table 1 for concentrations of individual components). Their average chain length (ACL) was smallest at 300 °C for *A. americana* and at 300 °C and 350 °C for *C. miniata*. Interestingly, the carbon preference index (CPI) calculated for the most abundant chain lengths remained very small for *A. americana* (maximum 0.23 at 400 °C), whereas for *C. miniata* the smallest CPI was 0.22 at 200 °C and the largest 1.12 at 400 °C (Table 3). α,ω-Alkanediols (C_{22}-C_{34}) were only identified for *A. americana*, and their concentration, both absolute and relative, decreased with increasing temperature with a constant ACL, and were absent from 350 °C onwards (Fig. 3, Table 2).

Concentrations of fatty acids (C_{16}-C_{36}) were highest at 200 °C for *A. americana* and at 350 °C for *C. miniata*. Overall, amounts of fatty acids did not show a consistent relation with temperature. Relatively largest proportions were recorded at 350 °C for both (Fig. 3). The ACL of the fatty acids deceased slightly between 200–400 °C, while a large drop was found at 450 °C for both species (Table 2). Similar to the alkanols, the CPI of the fatty acids remained small for *A. americana* between 200 and 400 °C, but increased from 0.30 to 1.00 between 400 and 450 °C, while a larger values were obtained for *C. miniata*, which increased to 0.90 and 0.95 at 400 and 450 °C, respectively (Table 3).

For both species, abundances of α,ω-alkanedioic acids (carbon chain length ranging from C_{27}-C_{34}) were absolutely and relatively highest at 200 °C. They were absent from 300 °C for *A. americana*, whereas at 400 °C for *C. miniata*, which was also richer in α,ω-alkanedioic acids than *A. americana* (Fig. 3). No particular shortening of their chains with temperature was observed (Table 2).

ω-Hydroxy fatty acids (C_{22}-C_{34}) were more abundant in *A. americana* than in *C. miniata*, and similar to *n*-alkanols and α,ω-alkanediols, their abundance as well as their ACLs decreased with increasing temperature (Fig. 3; Table 2). For *A. americana* they disappeared after 300 °C while for this occurred after 250 °C.

9,10,18-Trihydroxy C_{18} fatty acid was found in *C. miniata* at 200 °C only, whereas in *A. americana* also traces were observed at 250 °C (Fig. 3).

Concentrations of 2-methylketones (C_{19}-C_{37}) increased from 200 °C to 400 °C and decreased at 450 °C for *A. americana*, while for *C. miniata* their concentration peaked at 350 °C before decreasing to a very small trace at 450 °C, whereas they were absent at 500 °C and higher. Relatively the largest amounts of 2-methylketones were detected at 350 °C for both species (Fig. 3). Their ACLs were relatively constant for

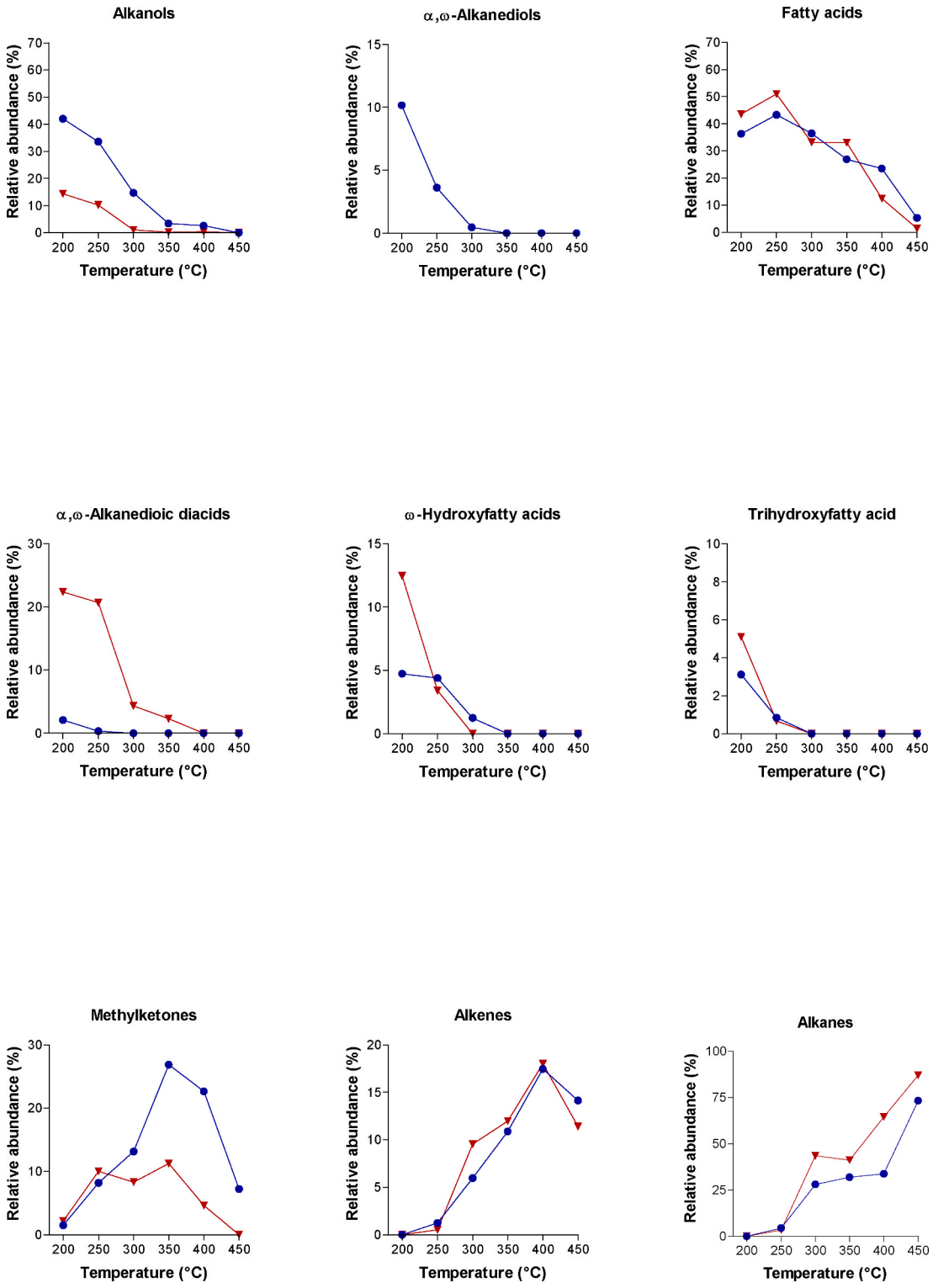


Fig. 3. Relative abundances of nine extractable component groups upon heating of cutan fractions from *A. americana* (●) and *C. miniata* (▼).

A. americana, whereas for *C. miniata* shortening was more pronounced (Table 2). A marked difference in CPI was observed between the two species: a gradual decrease form 10.0 to 1.6 over temperature was observed for *A. americana*, whereas for *C. miniata* the CPI increased from 1.7 at 200 °C to 2.3 at 300 °C, after which it decreased to 1.1 at 450 °C (Table 3).

While absent at 200 °C, the concentrations of *n*-alkenes (C_{20}-C_{34}) and *n*-alkanes (C_{18}-C_{37}) increased from 250 to 450 °C for both species, with *C. miniata* always being richer in both compound groups. However, at 500 °C they were either absent (*A. americana*) or detected in very small amounts (*C. miniata*). Also relatively the highest *n*-alkane amounts were found at 450 °C for both species, while for *n*-alkenes this was at 400 °C (Fig. 3). The ACL of the alkenes decreased with temperature for both species particularly at 450 °C, while for alkanes chain length shortening was smaller if any (Table 2). For both components the CPIs were between 0.5 and 1.6 for alkenes released from *A. americana*, and always

Table 1
Concentrations of the extractable compound classes after charring of cutan fractions for each temperature.

	A. americana						*C. miniata*					
Temperature (°C)	200	250	300	350	400	450	200	250	300	350	400	450
Compound class												
Concentration	ug g^{-1}	ug g^{-1}	ug g^{-1}	ug g^{-1}	ug g^{-1}	ug g^{-1}	ug g^{-1}	ug g^{-1}	ug g^{-1}	ug g^{-1}	ug g^{-1}	ug g^{-1}
Alkanols	396	687	352	142	225	0	243	139	33	14	43	0
α,ω-Alkanediols	96	74	11	0	0	0	0	0	0	0	0	0
Fatty acids	342	886	872	1120	2037	938	738	693	1055	2671	1427	606
α,ω-Alkanedioic acids	20	7	0	0	0	0	379	281	138	188	0	0
ω-Hydroxy fatty acids	45	90	30	0	0	0	218	62	0	0	0	0
9,10,18-Trihydroxy fatty acid	29	20	0	0	0	0	87	9	0	0	0	0
Methylketones	14	168	315	1119	1965	1283	36	136	265	911	530	4
Alkanes	0	92	671	1330	2931	12,977	0	47	1385	3333	7378	37,089
Alkenes	0	26	143	453	1515	2502	0	7	303	967	2060	4853
SUM	**942**	**2050**	**2364**	**4163**	**8673**	**17,700**	**1701**	**1376**	**3180**	**8084**	**11,438**	**42,552**

Table 2
Average Chain Length (ACL) of the extractable compounds with the chain length ranges indicated.

		A. americana						*C. miniata*					
	Temperature (°C)	200	250	300	350	400	450	200	250	300	350	400	450
Compound class	Chain length range												
Extracts													
Fatty acids (free and methyl esters)	16–36	30.5	30.7	30.6	29.6	29.7	21.5	31.7	29.7	30.1	29.7	28.3	21.3
Alkanols	22–34	30.1	29.4	29.4	29.7	30.5		31.4	29.0	29.0	31.1	30.7	
α,ω-Alkanediols	28–34	31.3	31.4	31.5									
α,ω-Alkanedioic acids	27–34	31.4	30.9					32.2	32.6	33.0	32.4		
ω-Hydroxy fatty acids	22–34	31.4	29.7	29.1				32.3	29.6				
Methylketones	19–37	31.3	31.4	31.8	31.3	31.6	31.0	32.7	31.2	32.0	31.4	31.3	30.9
Alkanes	18–37		29.0	28.2	28.5	29.3	29.0		29.2	29.4	29.0	30.2	28.7
Alkenes	20–34		29.6	28.5	29.7	29.8	27.3		30.0	29.4	28.5	29.5	27.0
Py-GC–MS													
Alkylbenzenes	4–34	19.2	20.0	17.7	19.2	16.4	18.8	23.4	23.1	19.0	18.2	19.5	17.4
Fatty acid methyl esters	7–34	27.6	27.3	25.9	27.2	26.0	24.9	27.5	29.2	25.9	24.7	17.4	
Methylketones	7–37	28.9	28.7	26.8	27.5	25.9	26.4	30.9	29.7	26.8	27.2	27.3	27.8
Unsat. methylketones	8–37	25.8	27.5	25.6	28.6	23.5		26.9	24.4	23.4	22.3	21.6	
Alkanes	9–37	23.7	24.0	24.2	24.2	22.2	22.4	26.5	25.9	24.8	23.5	23.5	22.2
1-Alkenes	9–37	22.1	21.7	22.3	22.7	20.6	21.0	23.2	22.1	22.2	20.2	20.7	19.8
α,ω-Alkadienes	9–37	21.3	21.1	22.4	22.3	21.5	20.9	23.2	22.5	22.3	20.2	20.6	20.5
THM													
Fatty acid methyl esters	7–34	26.6	25.5	27.3	23.3	21.8		22.8	22.4	20.5	23.8		
Methoxyalkanes	22–34	31.0	31.1	31.0	30.8	30.7		32.1	31.7	31.5	31.6		
α,ω-Dimethoxyalkanes	28–34	31.3	31.7	31.6	31.3	30.8		31.0	29.9		30.9		
ω-Methoxy fatty acid methyl esters	22–34	30.9	30.9	30.6	30.6			31.9	30.3	31.5	30.8		
Alkadiene/alkene/alkane triplets	20–35	28.3	28.5	27.0	27.8	27.5		30.3	29.4	28.2	29.3		

Table 3
Carbon Preference Indices (CPIs) of the extractable compounds with the chain length ranges indicated.

		A. americana						*C. miniata*					
	Temperature (°C)	200	250	300	350	400	450	200	250	300	350	400	450
Compound class	Chain length range												
Fatty acids	27–33	0.08	0.15	0.13	0.18	0.30	1.00	0.45	0.68	0.60	0.66	0.90	0.95
Alkanols	27–33	0.05	0.09	0.14	0.14	0.23		0.22	0.61	0.46	0.58	1.12	
α,ω-Alkanediols	29–33	0.17	0.14	0.14									
α,ω-Alkanedioic acids	29–33	0.64	0.92					1.13	1.19	0.70	0.70		
ω-Hydroxy fatty acids	27–33	0.23	0.51	0.51				0.19	0.59				
Methylketones	27–35	10.0	9.1	8.6	5.3	2.9	1.6	1.7	1.8	2.3	1.6	1.2	1.1
Alkanes	27–33		0.7	0.9	0.8	1.0	1.0		1.0	0.9	0.9	1.0	1.1
Alkenes	27–33		1.6	1.2	0.7	0.5	0.9		1.0	1.3	1.1	1.1	1.2

near 1.0 for alkanes derived from *A. americana* and both alkenes and alkanes generated thermally from *C. miniata* (Table 3). Not only 1-alkenes were found, also *cis* and *trans* 2-alkenes in smaller abundances were identified at 400 °C while absent from 300 °C and higher. For example, the ratio of the isomers 1-: *cis* 2-: *trans* 2- C_{32} alkene was 81.4: 5.2: 13.4 for *A. americana*, and 69.5: 8.0: 22.5 for *C. miniata* at 400 °C.

To investigate whether methanol, used several times during cutan isolation, was involved in the generation of in particular 2-methylketones, this solvent was replaced by ethanol. No products, however, with ethyl groups, such as 3-ethylketones, or ethylated carboxylic acid moieties, were observed (Suppl. Figs. S1 and S2.

3.3. Pyrolysis–GC–MS

Detected pyrolysis products of the solid residues after extraction were grouped into eight compound classes: α,ω-alkadienes, 1-alkenes,

alkanes, saturated and unsaturated 2-methylketones, fatty acid methyl esters, alkylbenzenes and 1-pristene. 1-Alkenes and alkanes were the most abundant components in all pyrolysates (Fig. 4). Charring caused an increase in alkenes (especially in *C. miniata*, from 30 to 50%) and alkanes (especially in *A. americana*, from 30 to 45%; Fig. 4). For α,ω-alkadienes and alkylbenzenes there was no significant trend with charring temperature (Fig. 4). Saturated 2-methylketones decreased in both sequences, especially ≥300 °C, and unsaturated methylketones and fatty acid methyl esters also disappeared at 400–450 °C (Fig. 4). Prist-1-ene, the only isoprenoid hydrocarbon, was only detected in the *C. miniata* pyrolysates, from which it diminished with increasing charring temperature (Fig. 4).

The ACL of alkanes from the *C. miniata* pyrolysates showed a consistent decrease from 26.5 to 22.2 across the temperature range, whereas the ACL of the alkanes from *A. americana* increased slightly from 23.7 to 24.2 between 200 °C and 350 °C, before decreasing to 22.4. Similar but less significant trends were found for the α,ω-alkadienes and alkenes for both species (Table 2). The ACLs of the fatty acid methyl esters and saturated 2-methylketones also decreased across the temperature range, and also more pronounced for *C. miniata* than for *A. americana*. Only for *C. miniata*, the ACL of unsaturated 2-methylketones (200–400 °C) and alkylbenzenes (limited to C_4-C_{34}) decreased with increasing charring temperature.

3.4. THM–GC–MS

Employing THM, most of the peaks was accounted for by fatty acid methyl esters (*A. americana* and *C. miniata*), the α,ω-alkadiene/alkene/alkane triplets (*C. miniata*) and ω-methoxyalkanes (*A. americana*; Fig. 5). In *A. americana*, α,ω-dimethoxyalkanes were also significant; both sequences produced some ω-methoxy fatty acid methyl esters and *C. miniata* produced traces of 9,10,18-trimethoxy C_{18} fatty acid methyl ester. Because the chromatograms of many high-temperature chars were of insufficient quality (450 °C of both species, 400 °C of *C. miniata*), trends with temperature were less clear than for pyrolysis–GC–MS, but it seemed that especially the ω-methoxy fatty acid methyl esters and α,ω-dimethoxyalkanes diminished due to charring whereas the ω-methoxyalkanes increased (Fig. 5). No major changes in chain length were observed, apart from a decline for the fatty acid methyl esters from *A. americana* (Table 2).

3.5. PCA

PC1 of the extractable compounds explained 43% with even long even numbered fatty acids, *n*-alkanols, ω-hydroxy fatty acids and α,ω-alkanedioic acids, and in particular alkenes and alkanes. PC1 scores increase with increasing charring temperature, PC2 represented 2-methylketones, α,ω-alkanediols, and shorter and odd numbered fatty acids for 22% and PC3 comprised α,ω-alkanedioic acids 13%. PC2 scores increase until higher temperature for *A. americana* than *C. miniata* (Fig. 6).

The PCA of the pyrolysis-GC–MS products yielded a PC1 that explained 33% of total variance. The PC1 scores show that PC1 reflected the overall trend of impact of charring in the whole temperature range (200–450 °C; Fig. 6). Loading patterns showed that charring intensity caused loss of mainly long-chain compounds (loadings < -0.5: C_{27}-C_{32} alkanes, C_{29}-C_{33} α,ω-alkadienes, 1-alkenes and alkanes, C_{27}-C_{32} saturated 2-methylketones, C_{26}-C_{32} alkylbenzenes) and fatty acids in general (C_{17}-C_{34}), whereas short-chain alkenes and alkanes (not α,ω-alkadienes) increased (Fig. 6). PC2 (20%) marked the difference between the two species, especially below 400 °C (at 400–450 °C, *C. miniata* and *A. americana* chars have similar PC2 scores). The PC2 loadings indicated that *A. americana* (negative loadings) was enriched in C_{11}-C_{30} α,ω-alkadienes, C_{27}-C_{29} alkenes, C_5-C_{21} alkylbenzenes and C_9-C_{27} 2-methylketones (saturated and unsaturated), whereas *C. miniata* had higher proportions of the C_{33}-C_{36} triplets and C_{29}-C_{34} alkylbenzenes. PC3 scores did not show clear trends.

For THM-GC–MS, PC1 (50%) illustrated the species difference, which again proved to be less explicit at higher temperatures (Fig. 6). PC1 loading patterns showed that *A. americana* is enriched in C_{11}-C_{27} fatty acids and the α,ω-alkadiene/alkene/alkane triplets, whereas *C. miniata* had larger proportions of particularly C_{30}-C_{32} fatty acids, C_{28}-C_{33} alkanols, C_{28}-C_{32} ω-hydroxy fatty acids and C_{26}-C_{34} α,ω-alkanediols. PC2 expressed the main thermal alteration trend (24%): the loss (positive loadings) of long-chain compounds (C_{33}-C_{34} fatty acids, C_{34} alkanol, C_{34} ω-hydroxy fatty acids and C_{30}-C_{35} triplets) and the increase (negative loadings) of C_{19}-C_{28} fatty acid methyl esters and C_{26}-C_{31} alkanols (Fig. 6). Hence, the THM fingerprints were more strongly affected by species than by charring, and the charring effect is mainly the shortening of the chain lengths of fatty acids and alkanols, and enrichment of alkanols in general. PC3 was mainly noise (9%).

4. Discussion

4.1. Weight loss

A comparison of the weight loss of charred cutan fractions from *A. americana* and *C. miniata* with experimental chars from other biopolymers, biomass or coals produced under the exact same conditions (double-wrapped in aluminium foil and charred for 30 min in a muffle furnace; Fig. 1) shows that: the cutans are 1) thermally more stable at all temperatures except for 600 °C than gorse wood (Martín-Seijo et al., 2021) and red mangrove wood (Kaal et al., 2012a), and Spanish moss (Kaal and Gilmore, 2018), with particularly large differences within the 250 °C to 450 °C range; 2) more stable than condensed tannins isolated from pine needles (Kaal et al., 2012b), especially in the 200–400 °C range; 3) less stable than a series of coal samples from Borneo (Kaal et al., 2017) especially at >400 °C with exception of the more immature coal at 200 °C and 300 °C. These results highlight the comparatively high thermal stability of the predominantly ester-bound aliphatic building blocks of cutan, especially <450 °C.

4.2. Hydroxy-and/or carboxylic acid-containing components

While the weight loss of cutan of both species exhibited a very similar thermal behaviour, both concentrations and composition of the compounds released were very different. Such different thermal behaviour was also the case for THM applied to isolated cutan. THM of cutan from *C. miniata* suffered from competition by conventional flash pyrolysis in the pyrolyser whereas that of *A. americana* did not: THM at 350 °C released the cutan building blocks in case of *A. americana*, while virtually nothing was produced from that of *C. miniata*. For the latter, THM at 510 °C or 600 °C yielded methylated cutan building blocks along with α,ω-alkadiene/1-alkene/alkane triplets (Leide et al., 2020).

Based on the study by Leide et al. (2020), the cutan from *A. americana* is dominated by C_{32} members within four compound classes, which, in decreasing order, are fatty acids, *n*-alkanols, α,ω-alkanediols, and ω-hydroxy fatty acids. At 200 °C, *n*-alkanols were slightly higher than the fatty acids, but at the higher temperatures 250–450 °C fatty acids consistently overshadowed the *n*-alkanols. The same holds for the α,ω-alkanediols vs. ω-hydroxy fatty acids (higher at 200 °C, and lower at 250 °C and 300 °C), implying that the acid functionality is better preserved upon heating, or that hydroxy groups are oxidized to carboxylic acid groups.

Both the thermally released components from cutan and the residual material as produced by THM from *C. miniata* contained a higher carboxylic acid/hydroxy ratio indicating that cutan had a different composition. The CPIs of the various compound groups, in particular those of *n*-alkanols and fatty acids, which were higher than that of *A. americana*, suggest that cutan from *C. miniata* is composed of a mixture of odd and even numbered moieties rather than predominantly even numbered ones of *A. americana*. Alternatively, given the more difficult production of THM compounds from *C. miniata* the structure of

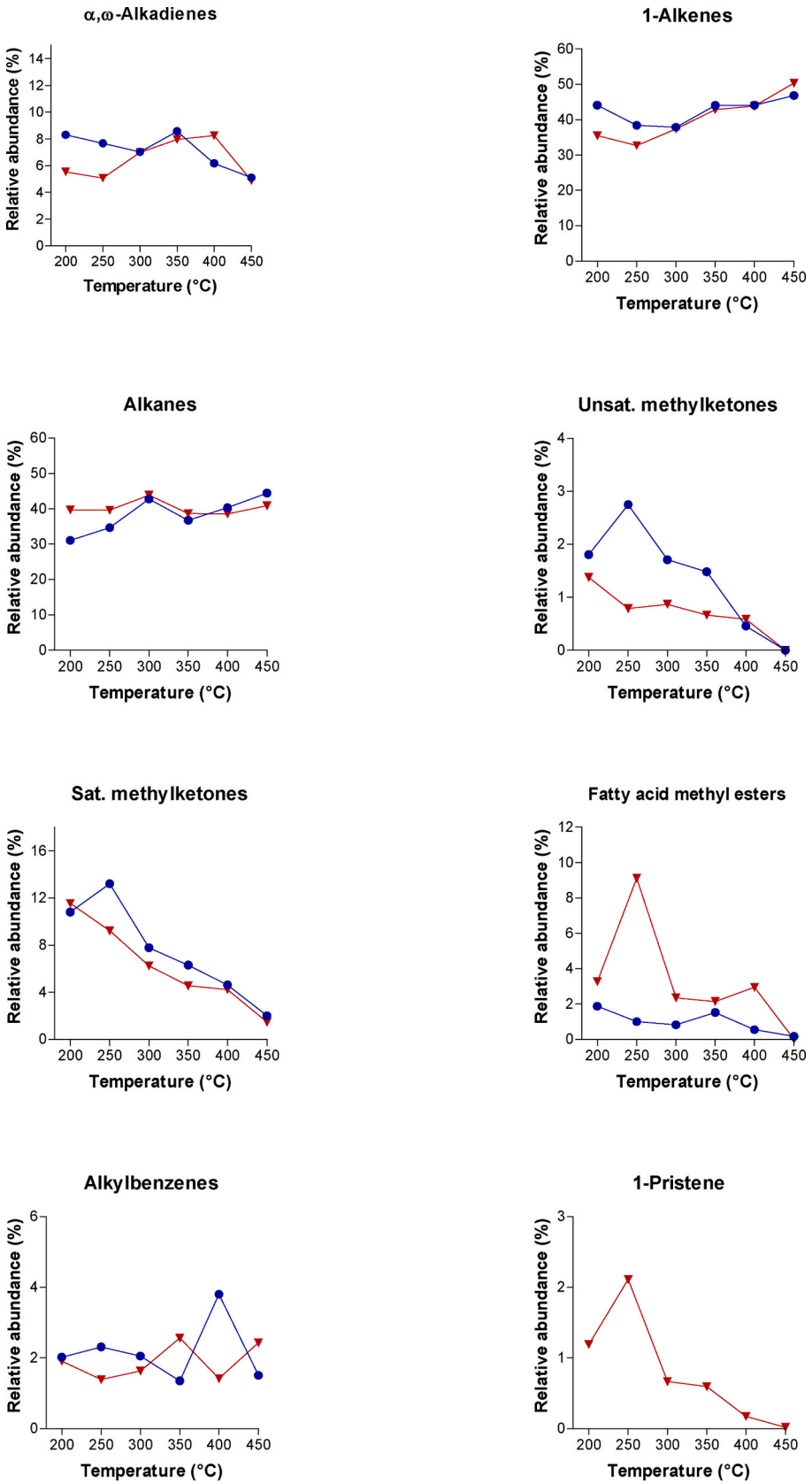


Fig. 4. Relative abundances of eight pyrolysis groups of cutan residues from *A. americana* (●) and *C. miniata* (▼) after extraction.

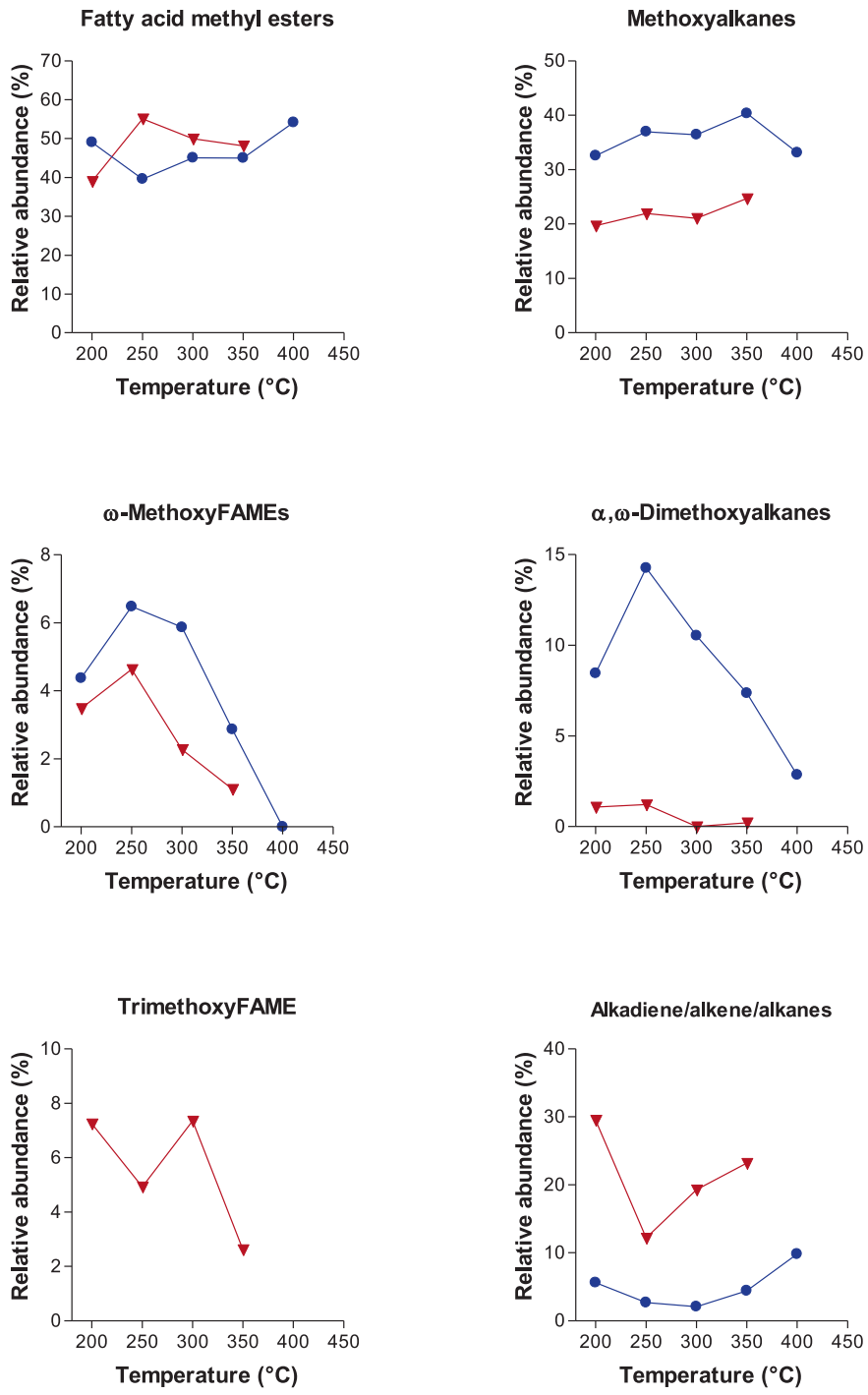


Fig. 5

Fig. 5. Relative abundances of six component groups of cutan residues from *A. americana* (●) and *C. miniata* (▾) upon THM after extraction.

cutan may be more thermally resistant through which the compounds that were released upon charring were cleaved more randomly compared to those from *A. americana* resulting in the enrichment of odd numbered *n*-alkanols and fatty acids.

The disappearance of α,ω-alkanedioic acids with increasing temperature indicates most likely decarboxylation resulting in the formation of fatty acids when one acid group is detached, or a hydrocarbon when both acids were removed. α,ω-Alkanedioic acids were not observed in cutan, while found in the cutin fractions of both species (Leide et al., 2020). Alternatively, hydroxy groups were oxidized during thermal alteration through which, for example, hydroxy fatty acids were converted to α,ω-alkanedioic acids.

9,10,18-Trihydroxy C_{18} fatty acid is indicative of traces of cutin that could not be released from the cutan fractions due to the strongly hydrophobic character of the material (Leide et al., 2020). 9,10,18-Trihydroxy fatty acid was found in *C. miniata* at 200 °C only, whereas in *A. americana* also traces were observed at 250 °C implying that heating was able to release residual cutin monomers from cutan, and hence that

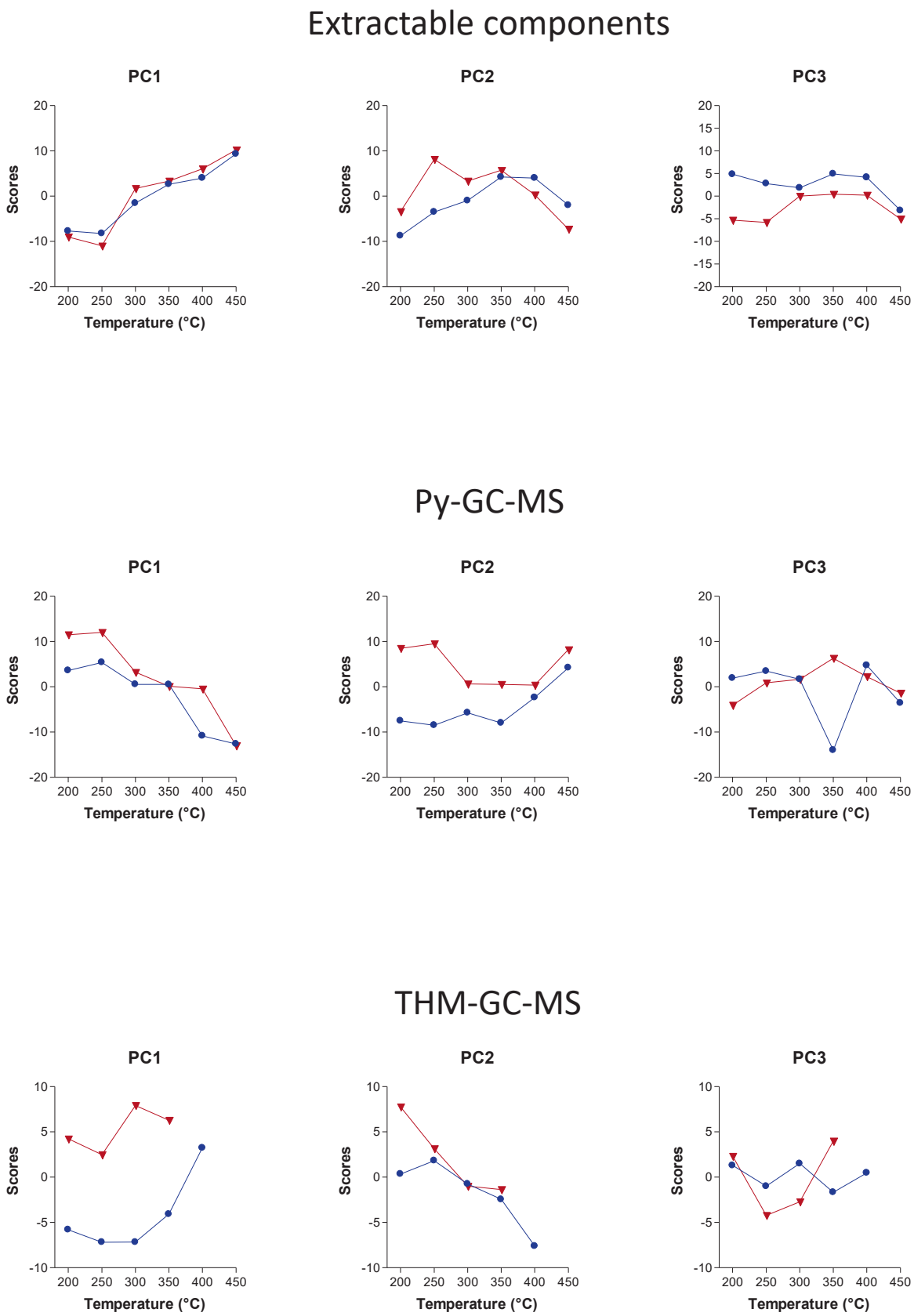


Fig. 6. Principal component analysis (PC1, PC2 and PC3) of extracts of charred cutan, pyrolysis products and THM products of cutan residues from *A. americana* (●) and *C. miniata* (▼).

relatively weaker bound moieties were released intact.

4.3. 2-Methylketones

The production of 2-methylketones upon heating of cutan, other aliphatic biopolymers and kerogen has been observed although primarily during flash pyrolysis studies (e.g. Tegelaar et al., 1989c, 1995; Boom et al., 2005; Zhang et al., 2016; Zhang and Volkman, 2020). Mid-chain ketones have been explained by the cleavage of ether bonds at corresponding positions (Gelin et al., 1993, Zhang et al., 2016). In that case, with only terminal acid and hydroxy groups present in the compounds observed, aldehydes instead of ketones would have been formed. Since we did not observe aldehydes, neither in the extractable fraction nor in the inextricable residues, their absence may be explained by any possible rearrangement(s) to form more stable 2-methylketones. Since the building blocks of cutan are mainly even numbered, predominantly even numbered 2-methylketones should be anticipated. However, the opposite is true: 2-methylketones observed have a strong odd-over-even predominance (in extracts, in residues). Cheng et al. (2018) propose that bacterially mediated methylation of aldehydes yields 2-methylketones. Such biotic pathway may be true in natural systems, but in our case not very likely. Could abiotic methylation have occurred during our experiment? Since we used methanol during extraction and saponification, it cannot be excluded that some methanol became trapped in the cutan fractions, which, subsequently, became involved in the thermally induced degradation of cutan. In order to investigate this possible route, cutan isolation using ethanol instead of methanol was conducted. Artificial heating of the resulting material at 300 °C did not reveal any 3-ethylketones, whereas 2-methylketones were still present in the extractable part of the thermally altered cutan fractions. Similarly, flash pyrolysis of the residues after extraction did not indicate any 3-ethylketones, while traces of 2-methylketones were observed. All together this implies that solvent used during cutan isolation was not involved in the production of 2-methylketones.

Based on the similar thermal behaviour of 2-methylketones they are likely derived from oxidized alkanol moieties, or alkyl chains cleaved upon thermal stress producing alkenes that were subsequently hydrated to 2-alkanols followed by oxidation (Obeid et al., 2015). The further increase of alkanes between 350 °C and 450 °C in expense of 2-methylketones and alkenes implies a continuous defunctionalisation and saturation of any generated alkyl chain. Although using a different technique, rather similar transformation were observed using hydrous pyrolysis, which artificially matures biomass, applied to bacteria (Jaeschke et al., 2008), algae (Obeid et al., 2015), leaves (Diefendorf et al., 2015) and aquatic ferns (Nierop et al., 2025).

4.4. (Un)saturated linear hydrocarbons

By lacking an (active) functional group, alkenes and alkanes were not present as such in the polymeric cutan network, and as they were not present in cutan at 200 °C also not likely incorporated. The CPI of the alkanes was also close to 1, mostly smaller rather than greater than 1. Hence, they were generated during artificial heating in a more or less similar way as such compounds were produced upon flash pyrolysis of cutan (Nip et al., 1986a; 1986b). However, while for flash pyrolysis homologous series of α,ω-alkadienes, 1-alkenes and alkanes, dominated by the alkenes, were observed, α,ω-alkadienes were not detected in the lipid extracts. The formation of 2-alkenes implies that the release of an alkyl chain, which produced a double bond, was performed under such conditions that double bond migration ('scrambling') took place, in a similar way as alkanols dehydrated into alkenes upon pyrolysis in the presence of clay minerals (Nierop and van Bergen, 2002).

Additionally, from 200 to 350 °C the concomitant generation of alkenes and in particular alkanes, both dominated by odd numbered chains (C_{29}, C_{31}) and demise of hydroxy and acid moieties suggests dehydration and decarboxylation of *n*-alkanols and fatty acids, respectively. Whether this defunctionalisation occurred before or after the release of the *n*-alkanols and fatty acids cannot be inferred from our data. The decreasing ACLs of the linear hydrocarbons, which was more pronounced during pyrolysis of the cutan residues, indicated the frequently observed chain-length shortening of aliphatic compound distribution upon charring (Wiesenberg et al., 2009; Kaal and Calvelo-Pereira, 2016).

4.5. Charring followed by pyrolysis and THM: twofold thermal degradation of cutan

We consider the charring experiments at temperatures ranging from 200 to 450 °C for 30 min as a slow and gentle thermal degradation process compared to flash pyrolysis and THM. Initially, charring caused the building blocks of cutan to be released without much change in ACLs implying rather intact building blocks. With increasing temperature modified building blocks (2-methylketones, alkanes and alkenes) appeared with relatively stable ACLs. By contrast, flash pyrolysis and THM showed that the molecular fingerprints of the residual cutan fractions were significantly altered as a result of charring. Charring affected not only the balance between main compound groups, but also their chain length distribution. Charring decreased the signals of long-chain members of many compound groups (fatty acids, alkylbenzenes, α,ω-alkanediols, ω-hydroxy fatty acids) and defunctionalisation of some of them: using Py-GC–MS, an increase in hydrocarbons at the expense of fatty acids; and using THM alkanols at the expense of ω-hydroxy fatty acids and α,ω-alkanediols.

Thermally released compounds during charring, and pyrolysis and THM of the cutan residues indicated that *C. miniata* produced larger proportions of long-chain members, i.e. alkylbenzenes and some α,ω-alkadiene/alkene/alkane triplets using Py-GC–MS; and fatty acids, *n*-alkanols and ω-hydroxy fatty acids for THM-GC–MS, whereas *A. americana* was enriched in short-chain members of those groups. Hence, the main difference between the species was the difference in chain length patterns. In addition, *A. americana* is composed of even numbered building blocks while than *C. miniata* produced more odd numbered analogues.

Contrary to expectations, none of the chars produced polycyclic aromatic hydrocarbons upon pyrolysis. The only detected typical products of pyrogenic organic matter were benzene and toluene (grouped with alkylbenzenes), with relative proportions always below 1% of quantified peak area. Such distribution indicates that polycondensation of aromatic groups is not a relevant charring mechanism of cutan. Nonetheless, the benzene/toluene ratio (Fig. 7), which has been used as an indicator of charring degree in biomass chars produced under the same experimental conditions (Suárez Abelenda et al., 2017), showed a significant increase with charring temperature for *A. americana*, possibly indicating incipient condensation. Finally, the pyrolysates did not reveal significant

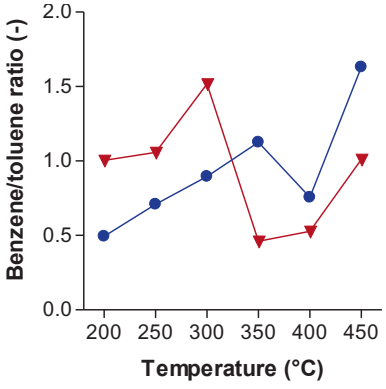


Fig. 7. Benzene/toluene ratio in pyrolysates of cutan residues from *A. americana* (●) and *C. miniata* (▼) after extraction.

peaks for branched alkanes and alkenes, which implied that formation of a branched network of hydrocarbon constituents is not a major thermal alteration pathway of the analysed cuticle ingredients, contrary to aliphatic-rich biomass materials (Suárez Abelenda et al., 2017).

5. Conclusions

Cutan isolated from both *A. americana* and *C. miniata* with very similar weight loss over 200–600 °C exhibited a different thermal degradation behaviour in terms of release of the building blocks and residual thermal degradation as assessed by flash pyrolysis and THM. Although composed of similar types of components, this implies that these components are chemically and/or physically differently configured and that cutan in *C. miniata* has on average longer building blocks. In addition, cutan of *C. miniata* is richer in moieties with acid functionalities than that of *A. americana*. With increasing charring temperature both the extractable (released) fraction and the residual part contained increasing amounts of 2-methylketones and saturated and unsaturated hydrocarbons, of which the latter two were indicative of defunctionalisation (dehydration and decarboxylation). For *A. americana* the compounds released at lower temperatures were more intact than that of *C. miniata* as indicated by their more pronounced CPIs. Charring as a process hardly affected the cutan structures, i.e., aromatization was limited, even at higher temperatures. This emphasizes the resistant nature of cutan fractions, which may potentially promote the preservation of cutan-containing cuticles in the fossil record. Over longer time scales and/or higher temperatures cutan may yield very long lipids – in particular of C_{28} and longer – ranging from fatty acids and alkanols, to 2-methylketones and eventually to alkenes and alkanes, hence, oil (like) production.

CRediT authorship contribution statement

Klaas G.J. Nierop: Writing – original draft, Resources, Methodology, Investigation, Formal analysis, Data curation, Conceptualization. **Joeri Kaal:** Writing – review & editing, Software, Methodology, Investigation, Formal analysis, Data curation, Conceptualization.

Declaration of competing interest

The authors declare that they have no known competing financial interests or personal relationships that could have appeared to influence the work reported in this paper.

Acknowledgements

The cuticles used in this study were kindly provided by Jana Leide (Julius-von-Sachs-Institute for Biosciences, University of Würzburg), which is highly appreciated. We thank Dick Kerver for the photo of the *Agave americana* plant in the Graphical Abstract, and the reviewers for their constructive comments.

Appendix A. Supplementary data

Supplementary data to this article can be found online at https://doi.org/10.1016/j.orggeochem.2026.105149.

Data availability

Data will be made available on request.

References

Boom, A., Sinninghe Damsté, J.S., De Leeuw, J.W., 2005. Cutan, a common aliphatic biopolymer in cuticles of drought-adapted plants. Organic Geochemistry 36, 595–601. https://doi.org/10.1016/j.orggeochem.2004.10.017.

Cheng, B., Xu, J., Liang, Y., Deng, Q., Tian, Y., Liao, Z., 2018. Determination and geochemical implication of multiple series of long-chain oxygen-bearing compounds trapped in kerogen in the Lucaogou formation, Santanghu Basin, NW China. Organic Geochemistry 121, 68–79. https://doi.org/10.1016/j.orggeochem.2018.04.005.

Deshmukh, A.P., Simpson, A.J., Hadad, C.M., Hatcher, P.G., 2005. Insights into the structure of cutin and cutan from *Agave americana* leaf cuticle using HRMAS NMR spectroscopy. Organic Geochemistry 36, 1072–1085. https://doi.org/10.1016/j.orggeochem.2005.02.005.

Diefendorf, A.F., Sberna, D., Taylor, D.W., 2015. Effect of thermal maturation on plant-derived terpenoids and leaf wax n-alkyl components. Organic Geochemistry 89, 61–70.

Gelin, F., Gatellier, J.-P.-L.-A., Sinninghe Damsté, J.S., Metzger, P., Derenne, S., Largeau, C., De Leeuw, J.W., 1993. Mechanisms of flash pyrolysis of ether lipids isolated from the green microalga *Botryococcus braunii* race A. Journal of Analytical and Applied Pyrolysis 27, 155–168. https://doi.org/10.1016/0165-2370(93)80006-L.

Gouret, E., Rohr, R., Chamel, A., 1993. Ultrastructure and chemical composition of some isolated plant cuticles in relation to their permeability to the herbicide, diuron. New Phytologist 124, 423–431. https://doi.org/10.1111/j.1469-8137.1993.tb03832.x.

Guzmán-Delgado, P., Graça, J., Cabral, V., Gil, L., Fernández, V., 2016. The presence of cutan limits the interpretation of cuticular chemistry and structure: *Ficus elastica* leaf as an example. Physiologia Plantarum 157, 205–220. https://doi.org/10.1111/ppl.12414.

Hall, G., Woodborne, S., Scholes, M., 2008. Stable carbon isotope ratios from archaeological charcoal as palaeoenvironmental indicators. Chemical Geology 247, 384–400. https://doi.org/10.1016/j.chemgeo.2007.11.001.

Jaeschke, A., Lewan, M.D., Hopmans, E.C., Schouten, S., Sinninghe Damsté, J.S., 2008. Thermal stability of ladderane lipids as determined by hydrous pyrolysis. Organic Geochemistry 39, 1735–1741. https://doi.org/10.1016/j.orggeochem.2008.08.006.

Kaal, J., Martínez Cortizas, A., Reyes, O., Soliño, M., 2012a. Molecular characterization of *Ulex europaeus* biochar obtained from laboratory heat treatment experiments – a pyrolysis-GC/MS study. Journal of Analytical and Applied Pyrolysis 95, 205–212. https://doi.org/10.1016/j.jaap.2012.02.008.

Kaal, J., Nierop, K.G.J., Kraal, P., Preston, C.M., 2012b. A first step towards identification of tannin-derived black carbon: conventional pyrolysis (Py-GC-MS) and thermally assisted hydrolysis and methylation (THM-GC-MS) of charred condensed tannins. Organic Geochemistry 47, 99–108. https://doi.org/10.1016/j.orggeochem.2012.03.009.

Kaal, J., Hasiah Abdullah, W., Makeen, Y., Azlan Mustapha, K., Asiwaju, L., Sia, S.-G., Almendros, G., 2017. Effects of maturity on the pyrolytic fingerprint of coals from North Borneo. International Journal of Coal Geology 182, 1–13. https://doi.org/10.1016/j.coal.2017.09.002.

Kaal, J., Gilmore, Z., 2018. Itla-okla (*Tillandsia osneoides*) fibre temper in Pre-Columbian ceramics. Journal of Analytical and Applied Pyrolysis APL002.

Kaal, J., Calvelo-Pereira, R., 2016. Pyrolysis-GC-MS of biochar, in: B. Singh, M. Camps-Arbestain, J. Lehmann (Eds.), Biochar: a Guide to Analytical Methods, CSIRO Publishing Melbourne, pp. 170–186. Doi: 10.1071/9781486305100.

Kolattukudy, P.E., 2001. Polyesters in higher plant,in: Scheper, T. (Ed.), Advances in Biochemical Engineering/biotechnology. Springer-Verlag, Berlin, Heidelberg, pp. 1–49. doi:10.1007/3-540-40021-4_1.

Leide, J., Nierop, K.G.J., Deininger, A.C., Staiger, S., Riederer, M., De Leeuw, J.W., 2020. Leaf cuticle analyses: implications for the existence of cutan/non-ester cutin and its biosynthetic origin. Annals of Botany 126, 141–162. https://doi.org/10.1093/aob/mcaa056.

Martín-Seijo, M., Kaal, J., Mayo, C., Mayo, J., 2021. Wood in pre-columbian funerary rituals: a case study from El Caño (Panama, AD 880–1020). Environmental Archaeology 26, 406–422. https://doi.org/10.1080/14614103.2020.1829301.

Nierop, K.G.J., Mijs, M., Dekker, R., Speelman, E.N., Lewan, M.D., De Leeuw, J.W., Reichart, G.J., 2025. Thermal stability of freshwater fern Azolla biomarkers as assessed by hydrous pyrolysis. Organic Geochemistry 205, 105008. https://doi.org/10.1016/j.orggeochem.2025.105008.

Nierop, K.G.J., van Bergen, P.F., 2002. Clay and ammonium catalyzed reactions of alkanols, alkanoic acids and esters under flash pyrolytic conditions. Journal of Analytical and Applied Pyrolysis 63, 197–208. https://doi.org/10.1016/S0165-2370(01)00154-1.

Nip, M., Tegelaar, E.W., Brinkhuis, H., De Leeuw, J.W., Schenck, P.A., Holloway, P.J., 1986a. Analysis of modern and fossil plant cuticles by Curie point Py-GC and Curie point Py-GC-MS: recognition of a new, highly aliphatic and resistant biopolymer. Organic Geochemistry 10, 769–778. https://doi.org/10.1016/S0146-6380(86)80014-6.

Nip, M., Tegelaar, E.W., De Leeuw, J.W., Schenck, P.A., Holloway, P.J., 1986b. A new non-saponifiable highly aliphatic and resistant biopolymer in plant cuticles: evidence from pyrolysis and ^{13}C-NMR analysis of present-day and fossil plants. Naturwissenschaften 73, 579–585. https://doi.org/10.1007/BF00368768.

Obeid, W., Salmon, E., Lewan, M.D., Hatcher, P.G., 2015. Hydrous pyrolysis of *Scenedesmus* algae and algaenan-like residue. Organic Geochemistry 85, 89–101. https://doi.org/10.1016/j.orggeochem.2015.04.001.

Rakotomalala, R., 2005. TANAGRA: a free software for research and academic purposes. Proceedings of EGC, RNTI-e-3, pp. 697–702. http://eric.univ-lyon2.fr/~ricco/tanagra/en/tanagra.html.

Schmidt, H.W., Schönherr, J., 1982. Development of plant cuticles: occurrence and role of non-ester bonds in cutin of *Clivia miniata* Reg. leaves. Planta 156, 380–384. https://doi.org/10.1007/BF00397478.

Schouten, S., Moerkerken, P., Gelin, F., Baas, M., De Leeuw, J.W., Sinninghe Damsté, J. S., 1998. Structural characterization of aliphatic, non-hydrolyzable biopolymers in

freshwater algae and a leaf cuticle using ruthenium tetroxide degradation. Phytochemistry 49, 987–993. https://doi.org/10.1016/S0031-9422(97)00942-4.

Shechter, M., Xing, B., Chetetz, B., 2010. Cutin and cutan biopolymers: their role as natural sorbents. The Soil Science Society of America Journal 74, 1139–1146. https://doi.org/10.2136/sssaj2009.0313.

Suárez Abelenda, M., McBeath, A., Kaal, J., 2017. Translating analytical pyrolysis fingerprints to thermal Stability Indices (TSI) to improve biochar characterization by pyrolysis-GC-MS. Biomass and Bioenergy 98, 306–320. https://doi.org/10.1016/j.biombioe.2017.01.021.

Tegelaar, E.W., De Leeuw, J.W., Derenne, S., Largeau, C., 1989a. A reappraisal of kerogen formation. Geochimica et Cosmochimica Acta 53, 3103–3106. https://doi.org/10.1016/0016-7037(89)90191-9.

Tegelaar, E.W., Matthezing, R.M., Jansen, J.B., Horsfield, B., De Leeuw, J.W., 1989b. Possible origin of *n*-alkanes in high-wax crude oils. Nature 342, 529–531. https://doi.org/10.1038/342529a0.

Tegelaar, E.W., De Leeuw, J.W., Largeau, C., Derenne, S., Schulten, H.-R., Müller, R., Boon, J.J., Nip, M., Sprenkels, J.C.M., 1989c. Scope and limitations of several pyrolysis methods in the structural elucidation of a macromolecular plant constituent in the leaf cuticle of *Agave americana* L. Journal of Analytical and Applied Pyrolysis 15, 29–54. https://doi.org/10.1016/0165-2370(89)85021-1.

Tegelaar, E.W., Hollman, G., Van der Vegt;, P., De Leeuw, J.W., Holloway, P.J., 1995. Chemical characterization of the periderm tissue of some angiosperm species: recognition of an insoluble, non-hydrolyzable, aliphatic biomacromolecule (Suberan). Organic Geochemistry 23, 239–250. https://doi.org/10.1016/0146-6380(94)00123-I.

Walton, T.J., 1990. Waxes, cutin and suberin. In: Harwood, J.L., Bowyer, J.R. (Eds.), Methods in Plant Biochemistry 4. Academic Press, London, pp. 105–158. https://doi.org/10.1201/9781351074070-5.

Wiesenberg, G.L.B., Lehndorff, E., Schwark, L., 2009. Thermal degradation of rye and maize straw: lipid pattern changes as a function of temperature. Organic Geochemistry 40, 167–174. https://doi.org/10.1016/j.orggeochem.2008.11.004.

Zhang, Z., Volkman, J.K., 2020. Isotopically enriched *n*-alkan-2-ones with even chain predominance in a torbanite from the Sydney Basin, Australia. Organic Geochemistry 144, 104018. https://doi.org/10.1016/j.orggeochem.2020.104018.

Zhang, Z.R., Volkman, J.K., Xie, X.M., Snowdon, L.R., 2016. Algaenan-derived midchain ketones from step-wise pyrolysis of the Huadian oil shale, NE China. Organic Geochemistry 91, 89–99. https://doi.org/10.1016/j.orggeochem.2015.10.011.